 DOI: 10.1002/masy.201000075

A Detailed Polymerization Model for Cerenol® Polyols

Philipp A. Mueller, Edward R. Murphy, Bhuma Rajagopalan, John P. Congalidis, Aaron R. Minter*

Summary: A mathematical model of the acid catalyzed 1,3-propanediol polymerization has been developed. Two catalysts investigated include sulfuric acid and superacid (tetrafluoroethane sulfonic acid or triflic acid). Based on a detailed reaction mechanism, population and mass balance equations have been derived for small molecules as well as for polymeric species of numerous chain distributions, which are distinguishable in terms of protonation state and end group functionality. Due to the interaction of the sulfuric acid catalyst with the polymer ends, a novel, dual index polymer chain distribution was derived and implemented.

The model has been validated with various sets of experimental data obtained in a lab-scale reactor setup. Dynamic model outputs such as monomer concentration, molecular weight averages, unsaturated and sulfate end groups, water evaporation rate and sulfate middle groups have been compared with experimental data of sulfuric and super acid catalyzed polymerization runs. Very good agreement between model predictions and experimental data has been obtained for both catalyst systems over an extended range of conditions using the same set of model parameter values. It is worth noting that the model is also capable of predicting polymerization equilibrium.

Keywords: bio-PDO®; cerenol®; condensation polymerization; end group analysis; molecular weight distribution; moment equations, 1,3-propanediol; polycondensation; polyether; polymerization modeling; polyol; polytrimethylene ether glycol

Introduction

Advances in fermentation, extraction and chemical process technology are paving the way for renewably-sourced polymers such as polylactic acid (PLA) and polyglycolide to take the place of some of the traditional petrochemical based polymers. The general trend is clear, polymers are being successfully developed using both partially bio-derived to 100% renewably-sourced materials.[1–4] As discussed by Kurian[5] 1,3-propanediol (PDO) is produced by a large scale industrial fermentation process (over 100 million pounds per year) and is used as a component in the recently commercialized poly (trimethylene terephthalate) Sorona® polymer. Recently, a new family of polyethers derived also from 1,3-propanediol has been commercialized by DuPont.[6,7,8] As the PDO monomer is produced from a glucose fermentation process (Bio-PDO®), the resulting polytrimethylene ether glycol (PO3G or Cerenol®) is 100% renewably sourced. The polymer can be used as a key ingredient in a variety of elastomeric products such as spandex fibers, thermoplastic polyurethanes, copolyester elastomers and copolyamide elastomers.

Polytrimethylene ether glycol is made in the acid catalyzed polycondensation reaction of 1,3-propanediol as shown below.

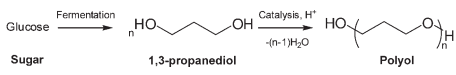

The polymerization yields water as a byproduct, which needs to be removed during the reaction in order to build polymer of sufficient molecular weight.

E. I. du Pont de Nemours and Company, Experimental Station, Wilmington, DE, 19880-0304, USA
Fax: (+1) 302 695 2504;
E-mail: philipp.a.mueller@usa.dupont.com

For the purpose of the study appropriate homogenous acid catalysts such as sulfuric acid and some sulfonic acids (''superacids'') have been used. Experimental efforts were focused on reducing cycle time by accelerating the polymerization without compromising on polymer properties in order to accelerate large-scale production and improve capital productivity.[9,10] A comprehensive reaction model incorporating both kinetics and mass transfer was developed in order to capture available kinetic data and to consolidate the learnings from process improvement efforts. This article highlights the model derivation and model validation with experimental data generated in a lab-scale reactor.

Experimental Part

This section outlines the experimental setup and the procedure used for carrying out the polymerizations of 1,3-propanediol to polytrimethylene ether glycol.

Experimental Setup

The experimental setup is depicted in Figure 1. The reactions were performed in a 1L glass kettle with baffles and a lid with multiple ports. An overhead mechanical stirrer with a pitched blade dual impeller was used to provide agitation. Polymerizations were carried out under a purge stream of an inert gas such as nitrogen. A heating mantle was used to achieve the reactor temperatures of interest. The temperature of the reaction mixture was controlled and monitored during the course of the run. An overhead condenser with a magnetically actuated valve was used to vary the reflux ratio of the condensate that was recycled back to the reactor. The temperature of the condenser was maintained using a circulating bath containing ethylene glycol/water mixture (50/50 v/v). The vapors leaving the condenser were subjected to further condensation in a couple of dry-acetone traps in series and stripped in a water column prior to venting. Samples of the distillate and polymer were collected at desired intervals and refrigerated prior to analysis. The reactions were carried out using two configurations: (a) with heat tracing wherein the reactor lid was heated to the reaction temperature and (b) without heat tracing wherein the reactor lid was at ambient conditions. Appropriate safety measures were taken to mitigate hazards

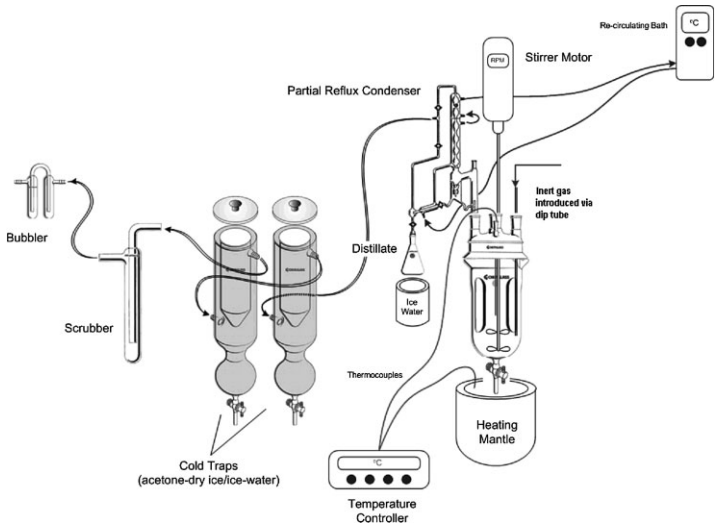

Figure 1.
Experimental setup for 1,3-propanediol polymerization.

relevant to the operation. The samples collected were analyzed using various analytical techniques such as NMR, Gas Chromatography and Karl-Fischer titration.

Experimental Procedure

The procedure for a typical run is summarized in this section. After the pre-startup checks to ensure the integrity of the setup, the monomer/catalyst solution is charged into the reactor. Inert gas is bubbled through the reactor under agitation at the desired rates and heating is initiated. The attainment of the reaction temperature is considered as the start of the reaction i.e. $t = 0$. The inert gas flow rates, agitation and temperature are monitored at specific intervals during the course of the run. Samples from the reactor and distillate are collected at desired time intervals. At the end of the reaction time, the reactor heating is terminated and the reactor contents are allowed to cool to ambient conditions. The contents of the reactor are removed and weighed. Weights of all samples collected, accumulated material in the dry ice traps and the residual material at the end of the run are recorded to account for mass balance closures. Typically $99 \pm 2\%$ mass balance closures were obtained. All exposed parts of the reactor are cleaned with an organic-aqueous mixture such as methanol-water solution, in preparation for the next run.

Model Development

A detailed kinetic mechanism for the superacid and sulfuric acid catalyzed Cerenol® polymerization has been proposed and is shown in Figure 2. It can be seen that the main polycondensation reaction occurs either via S_N1 or via S_N2 reaction type wherein the former involves the formation of a carbocation. Additional reactions forming sulfate end groups and sulfur middle groups can occur in the presence of sulfuric acid as shown in the top part of Figure 2. Moreover, unsaturated chain ends can be formed by E1 or E2 elimination reactions which can lead to color formation.

In order to properly account for all reactions taking place in this polymerization system and to maintain a minimum

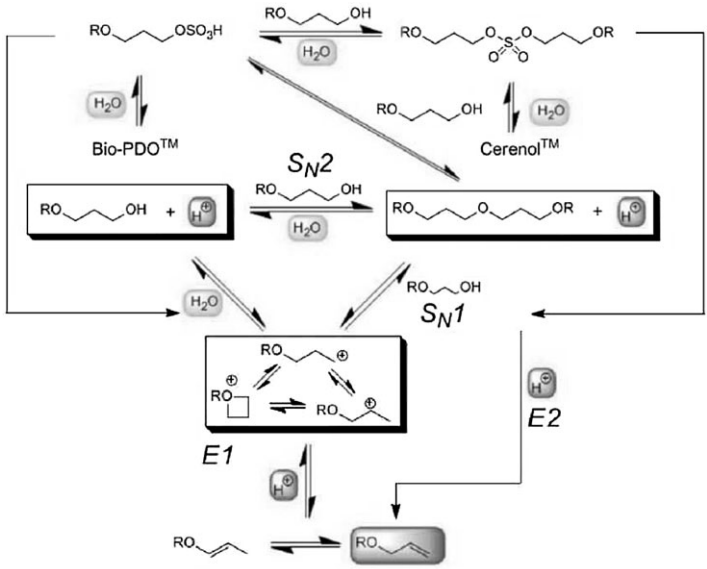

Figure 2.
Proposed reaction mechanism for sulfuric acid and superacid catalyzed Cerenol® polymerization.

amount of information that allows for the prediction of important polymer properties such as molecular weight distribution, unsaturated end groups and sulfate middle groups, the species listed in Figure 3 are included in the model. In order to account for protonation state and all different combinations of end groups, 27 polymer distributions are required. Moreover, two indices are used to describe the chain length distribution of the polymer, i.e. the number of ether linkages and the number of sulfur middle groups, respectively. It is worth noting that for coding reasons the indices counting ether and sulfate linkages are running from unity to infinity. Thus, a neutral chain made of two ether links and zero sulfur links (and capped with an alcohol group on each end) is written as *oDo*(3,1). *oDo*(1,1) denotes the monomer (1,3-propanediol). Degree of polymerization is therefore one plus the sum of ether and sulfate links or in terms of indices:

$$n = k + m - 1$$

with k and m being the indices counting ether and sulfate links, respectively.

Kinetics

Based on the mechanism in Figure 2 the elementary reaction steps listed in the following are included in the model. As mentioned previously, polymer chains are described by two indices, the first one denotes the number of ether (k or l) and the second the number of sulfate linkages (m or n), respectively. A list of model species used in the model is given in Figure 3.

Protonation: $$Base_i + H{-}Base_j \underset{k_{p,ji}}{\overset{k_{p,ij}}{\rightleftarrows}} H{-}Base_i + Base_j$$

It is worth noting that according to this reaction any component in its basic form can be protonated by any other component in its acidic form. A list of base/acid pairs accounted for in the model is given in Figure 4.

Carbocationformation :

$$xOPo(k,m) \underset{k'_{C+,1}}{\overset{k_{C+,1}}{\rightleftarrows}} xDp(k,m) + H_2O$$

$$xSPs(k,m) \underset{k'_{C+,2}}{\overset{k_{C+,2}}{\rightleftarrows}} xDp(k,m) + H_2SO_4$$

SN1:

$$xDp(k,m) + oDy(l,n) \underset{k'_{SN1,O}}{\overset{k_{SN1,O}}{\rightleftarrows}} xEPy(k+l, m+n-1)$$

$$xDp(k,m) + sDy(l,n) \underset{k'_{SN1,S}}{\overset{k_{SN1,S}}{\rightleftarrows}} xSEPy(k+l-1, m+n)$$

SN2 :

$$xOPo(k,m) + oDy(l,n) \underset{k'_{SN2,O}}{\overset{k_{SN2,O}}{\rightleftarrows}} xEPy(k+l, m+n-1) + H_2O$$

$$xSPs(k,m) + oDy(l,n) \underset{k'_{SN2,S}}{\overset{k_{SN2,S}}{\rightleftarrows}} xSEPy(k+l-1, m+n) + H_2O$$

E1 :

$$xDp(k,m) + Base_i \underset{k'_{E1}}{\overset{k_{E1}}{\rightleftarrows}} xDu(k,m) + H{-}Base_i$$

E2 :

$$xEPy(k+l,m+n-1) + Base_i \xrightarrow{k_{E2,O}} xDo(k,m) + yDu(l,n) + H-Base_i$$
$$xSEPy(k+l-1,m+n) + Base_i \xrightarrow{k_{E2,S}} xDs(k,m) + yDu(l,n) + H-Base_i$$

H_2SO_4 specific:

$$xDo(k,m) + H_2SO_4 \underset{k'_{sulf,1}}{\overset{k_{sulf,1}}{\rightleftarrows}} xDs(k,m) + H_2O$$
$$xSPs(k,m) + oDy(l,n) \underset{k'_{sulf,2}}{\overset{k_{sulf,2}}{\rightleftarrows}} xEPy(k+l,m+n-1) + H_2SO_4$$

Model assumptions

The following assumptions were made when developing the model:

- Step growth polymerization kinetics (condensation polymerization).
- All polymerization reactions take place in the liquid reactor phase only.
- Molecules and polymer chains cannot be protonated at more than one site at the same time.
- All kinetic rate coefficients are independent of chain length.
- Semi-empirical correlation is used for mass transfer coefficient.
- Sanchez-Lacombe equation of state is used to calculate phase behavior properties and phase partitioning.
- Ideal mixing (no concentration and temperature gradients within a given reactor phase).

Model Functionality

The experimental lab setup (cf. Figure 1) has been captured by the model as shown in Figure 5. The model setup essentially consists of the reactor vessel with vapor inlet (nitrogen and water), liquid inlet for reflux stream and vapor outlet for evaporation stream. The latter goes into the condenser, which is described as a single flash equilibrium stage. The effluent liquid flow from the condenser goes to a splitter where the reflux ratio can be adjusted. According to this scheme, model input are reactor temperature, pressure and volume, condenser temperature and pressure, nitrogen and water vapor feed rates as well as reflux ratio. Agitator stirring rate is an additional model input parameter as described later. It is worth noting that these input variables may be given dynamically as a function of time or static in

TFES	Deprotonated super acid
TFES-H	Super acid
HSO4	Deprotonated sulfuric acid
HSO4-H	Sulfuric acid
H2O	Water
H2O-H	Protonated water
$Base_u$	General basic form of component *k*
$Base_u$-H	General acidic form of component *k*
i-D-j(o,s)	*i* and *j* terminated neutral chain with *o* ether links and *s* sulfur links
i-OP-o(o,s)	*i* terminated OH-end-protonated chain with *o* ether links and *s* sulfur links
i-SP-o(o,s)	*i* terminated OSO3H-end-protonated chain with *o* ether links and *s* sulfur links
i-EP-j(o,s)	*i* and *j* terminated ether-link-protonated chain with *o* ether links and *s* sulfur links ($o \geq 1$)
i-SEP-j(o,s)	*i* and *j* terminated sulfur-link-protonatedchain with *o* ether links and *s* sulfur links ($s \geq 1$)
i-D+(o,s)	*i* terminated carbocation with *o* ether links and *s* sulfur links
Indices:	
i, j	*o* = OH-end, *u* = unsaturation end, *s* = OSO3H-end
o, s	Number of ether links, $o = (0,\infty)$, and sulfur links, $s = (0,\infty)$

Figure 3.
Nomenclature of species included in the model.

k	$Base_k$	$H\text{-}Base_k$
1	HSO4	HSO4-H
2	TFES	TFES-H
3	H2O	H2O-H
4	o-D-o(o,s)	o-OP-o(o,s)
5	o-D-u(o,s)	o-OP-u(o,s)
6	o-D-s(o,s)	o-OP-s(o,s)
7	o-D-s(o,s)	o-SP-s(o,s)
8	s-D-u(o,s)	s-SP-u(o,s)
9	s-D-s(o,s)	s-SP-s(o,s)
10	o-D-o(o,s)	o-EP-o(o,s)
11	o-D-u(o,s)	o-EP-u(o,s)
12	o-D-s(o,s)	o-EP-s(o,s)
13	u-D-u(o,s)	u-EP-u(o,s)
14	s-D-u(o,s)	s-EP-u(o,s)
15	s-D-s(o,s)	s-EP-s(o,s)
16	o-D-o(o,s)	o-SEP-o(o,s)
17	o-D-u(o,s)	o-SEP-u(o,s)
18	o-D-s(o,s)	o-SEP-s(o,s)
19	u-D-u(o,s)	u-SEP-u(o,s)
20	s-D-u(o,s)	s-SEP-u(o,s)
21	s-D-s(o,s)	s-SEP-s(o,s)

Figure 4.
List of base/acid pairs accounted for in the model.

terms of constant values. Besides predictions on polymer quality (molecular weight, end groups etc.) dynamic model output variables are evaporation flow rate, vapor and liquid exit flow rate, reflux flow rate and reactor phase compositions. Note that all output flows consist of mixtures of monomer, water and nitrogen, the compositions of which are also predicted by the model. Moreover, in agreement with the second assumption, all reactions considered in the model and listed above are assumed to take place in the liquid reactor phase only.

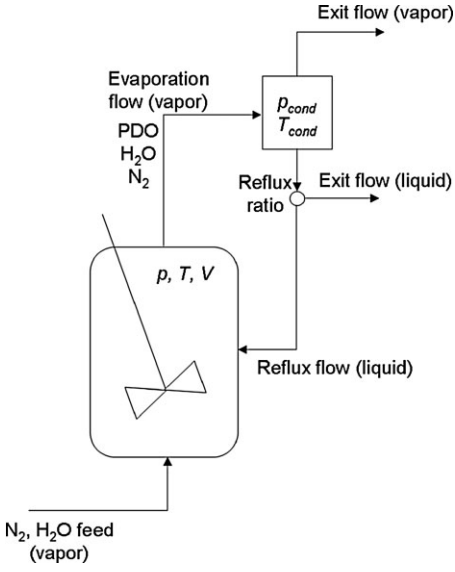

Figure 5.
Schematic view of the reactor setup as described by the model.

Phase Behavior

The Sanchez-Lacombe equation of state[11–14] together with the mixing rules reported by West et al.[15] have been used to describe phase behavior and phase partitioning in the reactor and in the condenser. In particular, given temperature and pressure flash algorithms have been solved in order to calculate interphase equilibrium partitioning of all components (i.e. monomer, water, and nitrogen) between liquid and vapor phases, except for catalyst and polymer, which are assumed to be present in the reactor liquid phase only. To calculate equilibrium partitioning a *p,T*-flash algorithm has been developed using the fugacity coefficient derived by Neau.[16]

Mass Transport

Under typical conditions and recipes for the Cerenol® polymerization reaction there are two phases coexisting in the reactor, a liquid phase mainly made of monomer, polymer, water and catalyst and a vapor phase predominantly consisting of monomer, water and nitrogen. Gaseous feeds are introduced into the liquid phase by using dip tubes. The total surface area of the resulting gas bubbles plays an important role for the rate of liquid-gas interphase mass transport.

Using the two-film theory[17,18] and assuming a dilute system the following general expression can be written for the molar flow rate of component *X* from liquid to gas phase:

$$\dot{N}_X = \left(\frac{1}{k_L a} + \frac{1}{m_X^{eq} k_V a}\right)^{-1} V_L \left([X_L] - \frac{[X_V]}{m_X^{eq}}\right)$$

where a is the interphase surface area per unit volume, V_L the volume of the liquid

phase, $[X_j]$ the concentration of X in phase j, m_X^{eq} the equilibrium partition coefficient and k_L and k_V the local mass transfer coefficients in the liquid and vapor phase, respectively. Assuming that diffusion in vapor is much faster than in liquid (i.e. $k_V >> k_L$), the above equation can be simplified:

$$\dot{N}_X = k_L a V_L \left([X_L] - \frac{[X_V]}{m_X^{eq}} \right)$$

A general mass transfer correlation for gas bubbles in a sparged tank reactor can be written as follows[19]:

$$k_L a = C \left(\frac{P}{V_L} \right)^x (v_G)^y$$

with P being power input, V_L liquid phase volume, v_G superficial gas velocity and C, x and y empirical parameters that can be estimated from correlating experimental data.

Mass Balances

The following mass balance equations are solved for component X in the reactor vapor phase:

$$\frac{dX_V}{dt} = \frac{\dot{m}_X^{IN,V}}{M_{m,X}} + k_L a V_L \left([X_L] - \frac{[X_V]}{m_X^{eq}} \right) - Q[X_V]$$

where X_V denotes number of moles, $[X_V]$ molar concentration, $\dot{m}_X^{IN,V}$ gaseous feed rate of component X in terms of mass per time, $M_{m,X}$ molecular weight, $k_L\,a$ the mass transfer coefficient as defined above, V_L volume of the reactor liquid phase, Q volumetric evaporation rate and m_X^{eq} the equilibrium partition coefficient defined as:

$$m_X^{eq} = \frac{[X_V^{eq}]}{[X_L^{eq}]}$$

where equilibrium concentrations in liquid and vapor phases are obtained from the solution of the pT-flash algorithm. Vapor phase mass balance equations are written for monomer, water and nitrogen. As mentioned previously, polymer and catalyst are assumed to be present in the reactor liquid phase only.

For a given component X in the reactor liquid phase we can write the following general mass balance equation:

$$\frac{dX_L}{dt} = \frac{\dot{m}_X^{IN,L}}{M_{m,X}} - k_L a V_L \left([X_L] - \frac{[X_V]}{m_X^{eq}} \right) + \sum_i r_X^i V_L$$

where $\dot{m}_X^{IN,L}$ is the liquid feed rate of component X in terms of mass per time and r_X^i the consumption/production rate of X due to reaction i. Liquid phase mass balance equations have been derived for monomer, water, nitrogen, catalyst as well as for all 27 polymeric species accounted for in the model.

Evaporation Rate

The actual amount of liquid phase and its composition are known from the solution of the liquid phase population balance equations. Using the Sanchez-Lacombe equation of state liquid phase density and volume can then be easily calculated. The available volume for the vapor phase in the reactor is given by the difference between total reactor volume (which is constant) and calculated liquid phase volume.

The evaporation flow rate Q is then adjusted in order to force the calculated vapor phase volume to match the available vapor phase volume. The calculated vapor phase volume is obtained by solving the equation of state using component amounts obtained from solving vapor phase mass balances. In this way a dynamically changing evaporation rate is predicted.

Moment Equations

The moment equations for the population balances are obtained through the moment generating function method.[20] It should be noted that the distribution is bivariate because two internal coordinates, i.e. the number of ether linkages k and the number of sulfate linkages m are considered. Moreover, as the number of sulfate linkages per chain is low (usually less than 10), the method of moments can only be applied to

ether links, whereas each distribution with a different number of sulfate middle groups must be considered individually. The derivation of these partial moments is not described in this manuscript.

The moment of order i with respect to ether linkages and order j with respect to sulfur middle groups of a given distribution is denoted with the same symbol as the chains of that distribution but marked with an asterisk. For instance, the moments of the distribution of neutral chains with an alcohol group on each end are defined as follows:

$$oDo^*_{ij} = \sum_{k=1}^{\infty}\sum_{m=1}^{\infty} k^i m^j oDo(k,m)$$

The differential moment equations are obtained by applying the above moment operator to the population balance equations:

$$\frac{d}{dt}\left(oDo^*_{ij}\right) = \sum_s r^s_{oDo^*_{ij}} V_L$$

Here, $r_{oDoi,j^*}{}^s$ is the production/consumption term of moment $oDo_{i,j}{}^*$ due to reaction s and calculated as follows:

$$r^s_{oDo^*_{ij}} = \sum_{k=1}^{\infty}\sum_{m=1}^{\infty} k^i m^j r^s_{oDo(k,m)}$$

The overall moment of order i with respect to ether linkages and order j with respect to sulfur middles is obtained by adding the moments of the same orders of all individual distributions accounted for in the model:

$$\begin{aligned}\mu_{ij} = {} & oDo^*_{ij} + oDu^*_{ij} + oDs^*_{ij} + uDu^*_{ij} \\ & + sDu^*_{ij} + sDs^*_{ij} + oEPo^*_{ij} + oEPu^*_{ij} \\ & + oEPs^*_{ij} + uEPu^*_{ij} + sEPu^*_{ij} + sEPs^*_{ij} \\ & + oSEPo^*_{ij} + oSEPu^*_{ij} + oSEPs^*_{ij} \\ & + uSEPu^*_{ij} + sSEPu^*_{ij} + sSEPs^*_{ij} \\ & + oOPo^*_{ij} + oOPu^*_{ij} + oOPs^*_{ij} \\ & + oSPs^*_{ij} + sSPu^*_{ij} + sSPs^*_{ij} + oDp^*_{ij} \\ & + uDp^*_{ij} + sDp^*_{ij}\end{aligned}$$

From the overall moments, number and weight average numbers of ether links and sulfur middles can be obtained as follows:

$$EL_n = \frac{\mu_{10}}{\mu_{00}} - 1 \quad EL_w = \frac{\mu_{20}}{\mu_{10}} - 1$$

$$SL_n = \frac{\mu_{01}}{\mu_{00}} - 1 \quad SL_w = \frac{\mu_{02}}{\mu_{01}} - 1$$

Number and weight average degree of polymerization as well as polydispersity index are then obtained from:

$$DP_n = EL_n + SL_n + 1$$

$$DP_w = EL_w + SL_w + 1$$

$$PD = \frac{DP_w}{DP_n}$$

Model Parameters

Two different approaches have been used to evaluate the large number of kinetic parameters included in the model:

- Literature values of acid dissociation constants and an assumed value for the forward reaction were used for the parameters required to describe protonation equilibria.
- Arrhenius parameters for the rate coefficients of all other reactions have been obtained by an optimization method.

The two estimation methods are detailed in the following.

Protonation reactions are assumed to be fast compared to all other reactions listed above, which means that protonation equilibria are reached instantaneously. This situation is achieved by assigning a value of 1.0×10^3 L/mol/s to all forward protonation rate coefficients, whereas the values of the reverse reactions have been evaluated from the equilibrium constants. For a general acid/base equilibrium reaction the equilibrium constant is obtained from the following expression:

$$K^{eq}_{p,ij} = \frac{k_{p,ij}}{k_{p,ji}} = \frac{[Base_i{-}H][Base_j]}{[Base_i][Base_j{-}H]}$$

where $k_{p,ij}$ and $k_{p,ji}$ are the rate coefficients of the forward and reverse reaction, respectively. If we consider H_2O for $Base_j$

we have:

$$K_{p,i3}^{eq} = \frac{k_{p,i3}}{k_{p,3i}} = \frac{[Base_i{-}H][H_2O]}{[Base_i][H_2O{-}H]} = \frac{[H_2O]}{K_{a,i}}$$

with $K_{a,i}$ being the acid dissociation constant of component *i*. Thus, for the general acid/base equilibrium constant we can write:

$$K_{p,ij}^{eq} = \frac{K_{p,i3}^{eq}}{K_{p,j3}^{eq}} = \frac{K_{a,j}}{K_{a,i}}$$

This means that the equilibrium constants of the protonation equilibria occurring in the Cerenol® reaction mixture can be estimated from the acid dissociation constants, which are available in the literature for a large number of components. Table 1 contains a summary of pK_a values used in the model.

Since no values of the rate coefficients were found in the literature for all other reactions considered in the model, these values have been adjusted in order to optimize agreement between model results and experimental data of selected polymerization runs. In particular, the parameter optimization was done in two steps. The first step consisted of manual adjustments of parameter values with the goal of minimizing differences between predicted and observed molecular weight average, unsaturated ends as well as sulfate ends. The obtained set of parameter values was then used as input for a least-square optimization algorithm (MATLAB function *lsqnonlin*).

Sanchez-Lacombe molecular and binary interaction parameters have been obtained by fitting pure component and mixture data. Pure component parameter values obtained for water and nitrogen are listed in Table 2.

Table 2.
Sanchez-Lacombe molecular parameters used in the model.

Component	T^*, *K*	p^*, *bar*	ρ^*, *kg/m³*
Water	626.6	26,674	1097.3
Nitrogen	148.4	1,656	895.6

Finally, the three parameters used in the mass transfer correlation have been obtained by fitting experimental data obtained at different stirring rate and nitrogen flow rate.

Results

Figures 6 and 7 summarize the comparison of model predictions with experimental data for two sulfuric acid catalyzed polymerization runs carried out in the lab reactor setup shown in Figure 1. Reaction parameters varied in these runs were condenser temperature, reflux ratio and water feed rate as shown in subfigures (a) and (b).

It can be seen that the agreement between calculated and observed data is very good in terms of reactor water concentration, evaporated amounts of water and monomer, molecular weight averages as well as unsaturated end group concentration.

Note that the polymerization run carried out with water addition approaches an equilibrium state as seen in Figure 7 (e). This is because water concentration in the reactor liquid phase reaches a steady state value after the first half of the batch due to constant water feed. The final molecular

Table 1.
pK_a values used in the model.

$Base_i$	$H\text{-}Base_i$	$pK_{a,i}$	Comments/source
HSO_4	$HSO_4\text{-}H$	−2.8	$H_2\ SO_4$: pK_a(25 °C) = -2.8 [21]
TFES	TFES-*H*	−12.0	Value between -12 and -15 [21]
$H_2\ O$	$H_2O\text{-}H$	−1.74	$H_3\ O^+$: pK_a(25 °C) = -1.74 [21]
∼OH	$\sim OH_2^+$	−1.94	$EtOH_2^+$: pK_a(25 °C) = -1.94 [22]
$\sim OSO_3H$	$\sim OSO_3H_2^+$	−3.0	assumed
∼O∼	$\sim OH^+\sim$	−2.39	$Et_2\ OH^+$: pK_a(25 °C) = -2.39 [22]
$\sim O(SO_2)O\sim$	$\sim O(SO_2)OH^+\sim$	−3.5	assumed

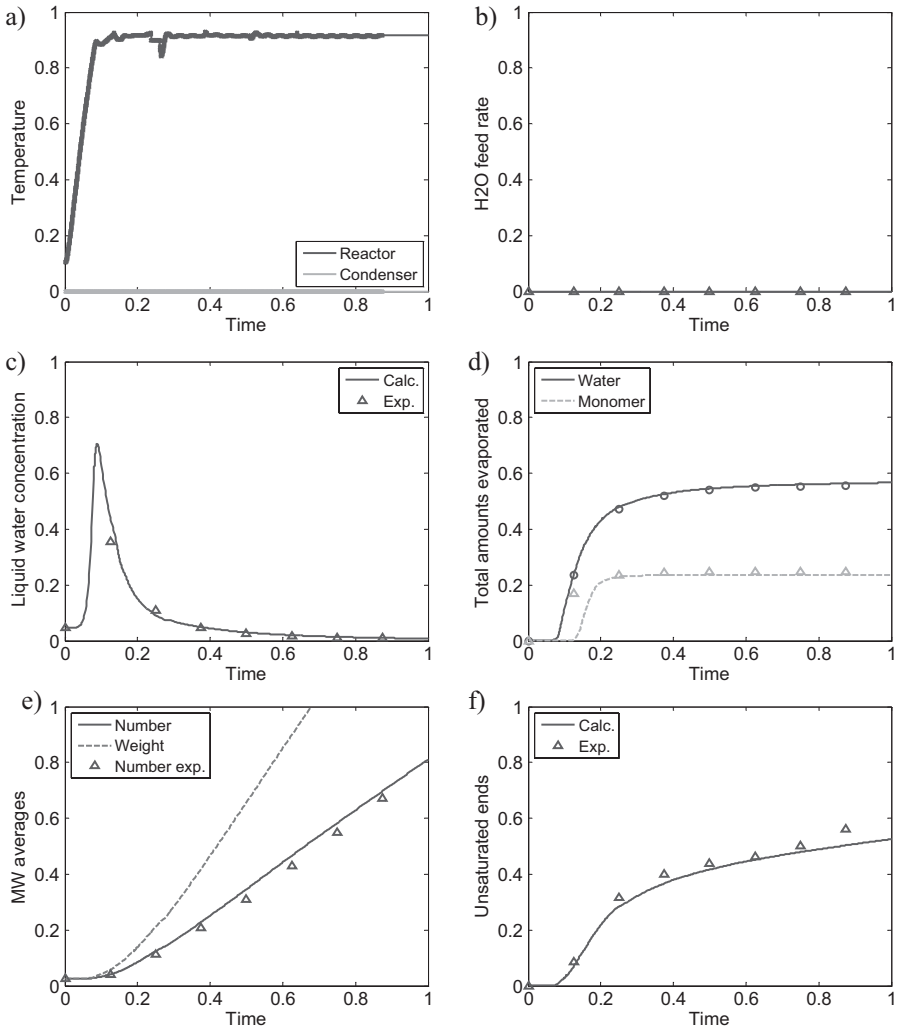

Figure 6.
Calculated (lines) and observed (symbols) data for sulfuric acid catalyzed run obtained under standard conditions without water addition and no reflux: (a) reactor and condenser temperature (input), (b) water feed rate (input), (c) reactor water concentration, (d) evaporated amounts of monomer and water, (e) molecular weight averages, (f) unsaturated end groups.

weight is close to the equilibrium molecular weight at the obtained water concentration.

In Figure 8 model results and experimental data for a superacid catalyzed polymerization run are shown. Good agreement is found between predicted and measured water concentration, molecular weight averages as well as unsaturated end groups. The effect of reducing reactor temperature on the time evolution of molecular weight and unsaturates is well reproduced by the model as seen in Figures 8 (e) and (f). It is worth noting that for this simulation run the same set of model parameters has been used as for the ones shown in Figures 6 and 7.

Conclusion

A reaction mechanism for the condensation polymerization of 1,3-propanediol to form

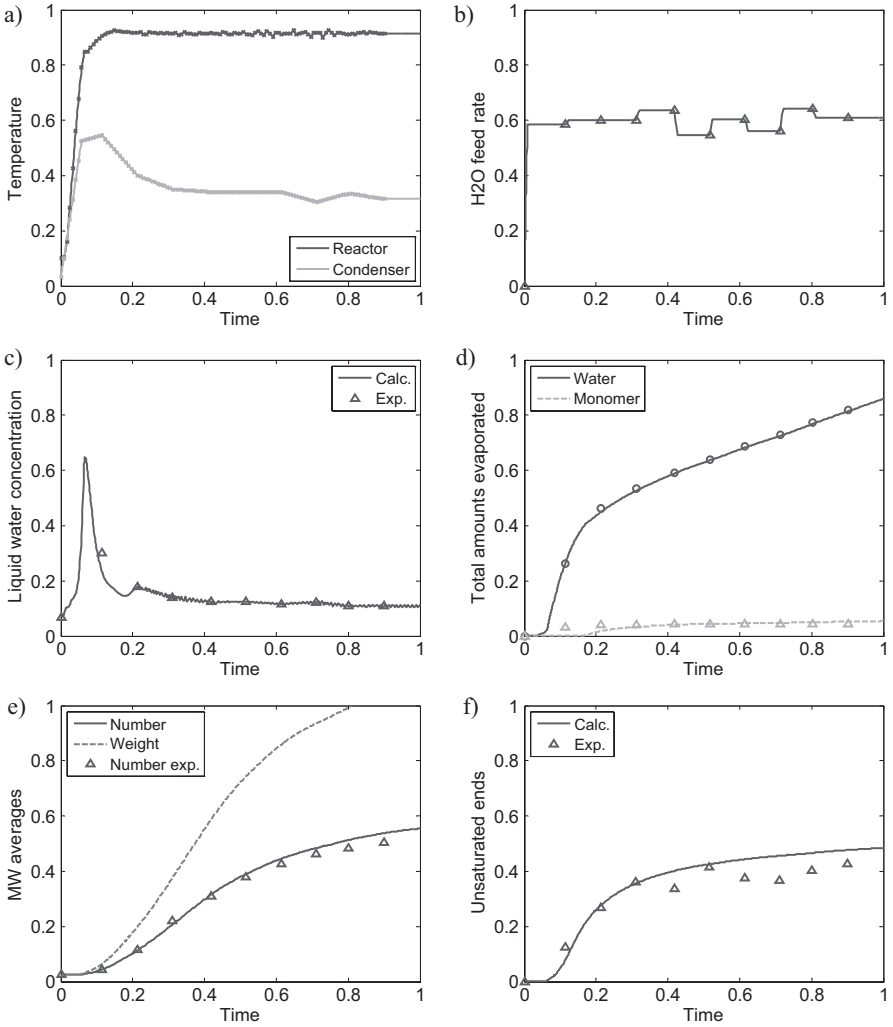

Figure 7.
Calculated (lines) and observed (symbols) data for sulfuric acid catalyzed run obtained under standard conditions with water addition and under partial reflux: (a) reactor and condenser temperature (input), (b) water feed rate (input), (c) reactor water concentration, (d) evaporated amounts of monomer and water, (e) molecular weight averages, (f) unsaturated end groups.

polytrimethylene ether glycol had been previously proposed for superacid catalyzed reactions. In this mechanism, S_N1 and S_N2 pathways compete for the consumption of monomer and alcohol terminated chains. The relative rates of these pathways are believed to be determined by temperature (due to differences in activation energies) and degree of protonation of alcohol and ether chains. The use of catalysts such as sulfuric acid further complicates the reaction mechanism due to its ability to get incorporated into the growing polymer chains as either sulfate linkages or sulfate terminated ends.

Based on the proposed mechanism a mathematical model has been developed including the description of a two-dimensional molecular weight distribution, interphase mass transport for the prediction of evaporation rates and the detailed description of chain end groups. Model results have

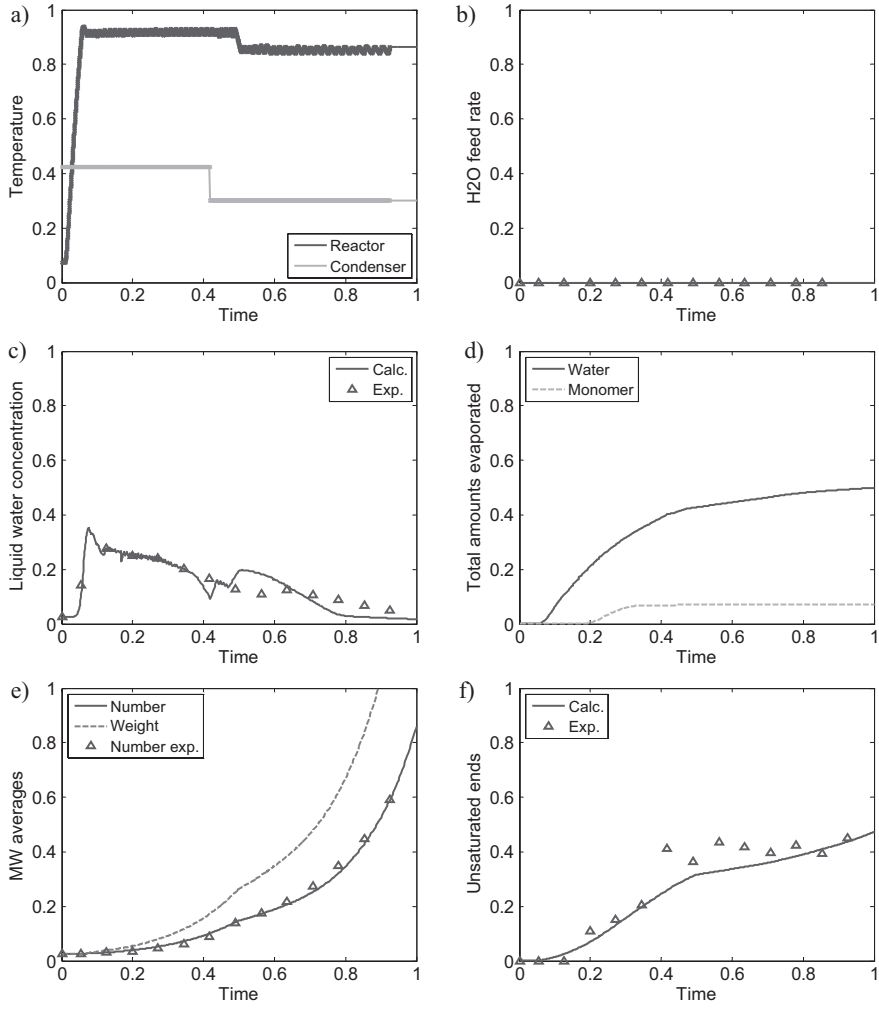

Figure 8.
Calculated (lines) and observed (symbols) data for superacid catalyzed run carried out with temperature ramp and under 100% reflux: (a) reactor and condenser temperature (input), (b) water feed rate (input), (c) reactor water concentration, (d) evaporated amounts of monomer and water, (e) molecular weight averages, (f) unsaturated end groups.

been successfully validated with experimental data obtained from both sulfuric acid and superacid catalyzed polymerization runs carried out under various conditions in a lab-scale reactor setup. This robust model can be used to evaluate process scale-up strategies and for improved process control.

[1] J. H. Clark, V. Budarin, F. E. I. Deswarte, J. J. E. Hardy, F. M. Kerton, A. J. Hunt, R. Luque, D. J. Macquarrie, K. Milkowski, A. Rodriguez, O. Samuel, S. J. Tavener, R. J. White, A. J. Wilson, *Green Chem.* **2006**, *8*, 853–860.

[2] J. Clark, F. Deswarte, "*Introduction to Chemicals from Biomass*", Wiley-VCH, **2008**.

[3] S. Fernando, S. Adhikari, C. Chandrapal, N. Murali, *Energy & Fuels* **2006**, *20*, 1727–1737.

[4] B. Gupta, N. Revagade, J. Hilborn, *Prog. Polym. Sci.* **2007**, *32*, 455–482.

[5] J. V. Kurian, in: "*Natural Fibers, Biopolymers, and Composites*", A. K., Mohanty, M., Misra, L. T. Drzal, Eds., CRC Press, **2005**, p. 497–525.

[6] H. B. Sunkara, R. W. Miller, "*DuPont™ Cerenol™ - A New Family of High Performance Polyether Glycols*", 5th Annual World Congress on Industrial Biotechnology & Bioprocessing, April 27-30, 2008, Chicago, IL, United States.

[7] T. Xie, ''Development of Bio-based Polymers: Fundamentals, Process Scale up and Technology Challenges for Cerenol^{TM}'', Polymer Reaction Engineering VII, May 3-8, 2009, Niagara Falls, Ontario, Canada.
[8] M. A. Harmer, D. C. Confer, C. K. Hoffmann, S. C. Jackson, A. L. Liauw, A. R. Minter, E. R. Murphy, R. E. Spence, H. B. Sunkari, *Green Chemistry*, in press
[9] M. A. Harmer, C. Hoffmann, S. C. Jackson, E. R. Murphy, R. Spence, ''*Preparation of polytrimethylene ether glycol or copolymers thereof*'', US Patent 20090118464 A1, **2009**.
[10] D. C. Confer, M. A. Harmer, C. Hoffmann, S. C. Jackson, S. S. Kristjansdottir, R. Spence, ''*Preparation of polytrimethylene ether glycol or copolymers thereof*'', US Patent 20090118465 A1, **2009**.
[11] I. C. Sanchez, R. H. Lacombe, *The Journal of Physical Chemistry* **1976**, *80*, 2352–2362.
[12] R. H. Lacombe, I. C. Sanchez, *The Journal of Physical Chemistry* **1976**, *80*, 2568–2580.
[13] I. C. Sanchez, R. H. Lacombe, *Polymers Letters Edition* **1977**, *15*, 71–75.
[14] I. C. Sanchez, R. H. Lacombe, *Macromolecules* **1978**, *11*, 1145–1156.
[15] B. L. West, D. Bush, N. H. Brandley, M. F. Vincent, S. G. Kazarian, C. A. Eckert, *Ind. Eng. Chem. Res.* **1998**, *37*, 3305–3311.
[16] E. Neau, *Fluid Phase Equilibria* **2002**, *203*, 133–140.
[17] W. K. Lewis, W. G. Whitman, *Industrial and Engineering Chemistry* **1924**, *16*, 1215–1220.
[18] R. H. Perry, D. W. Green, ''*Perry's Chemical Engineers' Handbook*'', 8th ed. McGraw-Hill, New York 2007, p. 5–59.
[19] R. H. Perry, D. W. Green, ''*Perry's Chemical Engineers' Handbook*'', 8th ed. McGraw-Hill, New York 2007, p. 5–76.
[20] N. A. Dotson, R. Galvan, R. L. Laurence, M. Tirrell, ''*Polymerization Process Modeling*'', VCH Publisher Inc., New York 1996.
[21] N. Furukawa, H. Fuijhara, in: ''*The chemistry of sulfonic acids, esters and their derivatives*'', S., Patai, Z. Rappoport, Eds., John Wiley & Sons, **1991**.
[22] G. Perdoncin, G. Scorrano, *Journal of the American Chemical Society* **1977**, *99*, 6983–6986.

